HHS Public Access

Author manuscript

FEBS J. Author manuscript; available in PMC 2015 July 01.

Published in final edited form as:

FEBS J. 2014 July ; 281(14): 3261–3279. doi:10.1111/febs.12859.

Muscle Lim Protein isoform negatively regulates striated muscle actin dynamics and differentiation

Elizabeth Vafiadaki[1], **Demetrios A. Arvanitis**[1,*], **Vasiliki Papalouka**[1,*], **Gerasimos Terzis**[2], **Theodoros I. Roumeliotis**[3,5], **Konstantinos Spengos**[4], **Spiros D. Garbis**[3,5], **Panagiota Manta**[4], **Evangelia G. Kranias**[1,6], and **Despina Sanoudou**[1,7]

[1]Molecular Biology Division, Biomedical Research Foundation of the Academy of Athens, Greece

[2]Athletics Laboratory, School of Physical Education and Sport Science, University of Athens, Greece

[3]Division of Biotechnology, Biomedical Research Foundation of the Academy of Athens, Greece

[4]1st Department of Neurology, University of Athens, School of Medicine, Eginition Hospital, Greece

[5]Cancer Sciences and Experimental Medicine, School of Medicine, University of Southampton, UK

[6]Department of Pharmacology and Cell Biophysics, College of Medicine, University of Cincinnati, Cincinnati, Ohio, U.S.A

[7]Department of Pharmacology, Medical School, National and Kapodistrian University of Athens, Greece

Abstract

Muscle Lim Protein (MLP) has emerged as a critical regulator of striated muscle physiology and pathophysiology. Mutations in cysteine and glycine-rich protein 3 (*CSRP3*), the gene encoding MLP, have been directly associated with human cardiomyopathies, while aberrant expression patterns are reported in human cardiac and skeletal muscle diseases. Increasing evidence suggests that MLP has an important role in both myogenic differentiation and myocyte cytoarchitecture, although the full spectrum of its intracellular roles has not been delineated. We report the discovery of an alternative splice variant of MLP, designated as MLP-b, showing distinct expression in neuromuscular disease and direct roles in actin dynamics and muscle differentiation. This novel isoform originates by alternative splicing of exons 3 and 4. At the protein level, it contains the N-terminus first half LIM domain of MLP and a unique sequence of 22 amino acids. Physiologically it is expressed during early differentiation, whereas its overexpression reduces C2C12 differentiation and myotube formation. This may be mediated through its inhibition of MLP/CFL2-mediated F-actin dynamics. In differentiated striated muscles, MLP-b localizes to the sarcomeres and binds directly to Z-disc components including α-actinin, T-cap and MLP. Our findings unveil a novel player in muscle physiology and pathophysiology that is implicated in

Correspondence: Despina Sanoudou, PhD, FACMG, Department of Pharmacology, Medical School, University of Athens, Mikras Asias 75, Athens 115-27, Greece, dsanoudo@enders.tch.harvard.edu, Tel : +30-210-7462712, Fax : +30-210-7462554.

*These authors contributed equally to this work

myogenesis as a negative regulator of myotube formation, and in differentiated striated muscles as a contributor to sarcomeric integrity.

Keywords

isoform; MLP; myotube differentiation; sarcomere; skeletal myopathy

Introduction

The cysteine and glycine-rich protein 3 (*CSRP3* or *CRP3)* gene codes for Muscle LIM Protein (MLP), a small 194 amino acid protein, which is specifically expressed in skeletal and cardiac muscles [1]. Accumulating evidence over the years has revealed a critical role for MLP in both striated muscle in physiology and pathophysiology. Mutations in *CSRP3* have been directly associated with dilated (DCM) and hypertrophic (HCM) cardiomyopathies [2–8], while aberrant expression levels of MLP have been found in human failing heart [9] and skeletal myopathies [10–12]. The absence of MLP, as shown in an MLP deficient mouse model, results in marked actin-cytoskeleton disorganization and disrupted cardiac myofibrillar cytoarchitecture, that may consequently lead to dilated cardiomyopathy and heart failure [13].

MLP is a member of the conserved LIM-only protein family and consists of two LIM functional zinc-finger domains, each followed by a glycine-rich domain [14]. LIM domain proteins are believed to function as adapters, facilitating macromolecular complexes [15–16]. Consistent with this, MLP has been demonstrated to bind to a number of different proteins, including telethonin (T-cap), α-actinin and cofilin-2 (CFL2) at the Z-disc, N-RAP at the intercalated disc, and also β-spectin at the costameres [6, 17–20]. Through its interactions with these structural proteins, MLP has been suggested to act as a scaffold protein for the sarcomere and the actin-based cytoskeleton [6, 13, 17–18, 21–22]. Based on its Z-disc distribution and on experimental evidence from the MLP knockout mouse model, MLP was proposed to be part of a macromolecular mechanical stretch sensor, suggesting a role in mechanosensation and mechanotransduction [6, 23]. In addition to this structural role, MLP has been shown to bind to transcription factors such as MyoD and Myogenin in the nucleus [24], and to promote myogenic differentiation [21]. However, the precise mechanism of action and the full spectrum of its intracellular roles remain elusive.

We report the discovery and characterization of a novel MLP protein isoform, designated herein as MLP-b, encoded by the *CSRP3* gene, that exhibits distinct roles in muscle differentiation and cytoarchitecture. The novel isoform MLP-b is significantly overexpressed in a variety of striated muscle disease patients, in agreement with recent findings that highlight the key role of gene isoforms' expression in striated muscle function regulation [25–26]. Functionally, MLP-b appears to act as a negative regulator of muscle differentiation, possibly through its negative regulation of the MLP-CFL2 mediated actin depolymerization. Furthermore, its Z disc localization and direct interaction with sarcomeric proteins suggests a functional role in sarcomere organization and integrity. Collectively,

these findings implicate MLP-b as a novel regulator of striated muscle, with important functions in both muscle physiology and pathophysiology.

Results

Identification of a novel isoform of MLP

RT-PCR analysis of CSRP3 in human cardiac and skeletal muscle cDNA resulted in detection of the full length CSRP3 cDNA (~660bp) and a fainter shorter product of ~400bp that represented a novel putative CSRP3 isoform (Fig. 1A). This putative isoform was also detected in a number of different skeletal muscle tissues, including quadriceps, deltoid, diaphragm and sternocleidomastoid muscles, confirming its mRNA expression and suggesting a role across different striated muscles (Fig. 1B). We next sought to investigate and define the exact composition and functional role of this newly identified MLP isoform in striated muscles. Initially, to determine the sequence of this isoform, the CSRP3 RT-PCR products were cloned in the TOPO TA vector, plasmids were isolated from the resulting clones and sequenced. Through bioinformatical analysis, the full length and isoform cDNA sequences were aligned and the common/unique regions were determined. This new isoform appears to be the product of alternative splicing of the full length CSRP3 mRNA resulting in skipping of exons 3 and 4. To evaluate the expression of this isoform at the protein level, western blot analysis was performed in cardiac and skeletal muscle protein extracts. In agreement with the mRNA findings, a smaller and less abundant MLP product was detected, in addition to the full length MLP (Fig. 1C), demonstrating that this alternatively spliced mRNA is translated to a protein product. Notably, this novel MLP isoform protein appears slightly larger than expected in size, possible reflecting conformational changes and/or post-translational modifications occurring within its unique amino acid sequence. To distinguish between the two forms of MLP, the full length MLP is referred to hereafter as MLP-a and the new, shorter, isoform as MLP-b.

In silico prediction of the protein product resulted in a 59 amino acid protein. Alignment of the newly identified isoform with the full length MLP determined that the N-terminus, including the first 37 amino acids, is identical between the two. However, the remaining 22 amino acids show no homology to MLP (Fig. 1D) as skipping of exons 3 and 4 through alternative splicing of the full length CSRP3 mRNA, leads to changes in the reading frame of the remaining transcript and ultimately to a different amino acid sequence. Interestingly, these 22 amino acids show no homology to any known proteins available in the public databases, as determined by BLAST analysis. Structurally, MLP-b is predicted to contain the first half LIM domain of full length MLP protein, followed by the unique 22 amino acid sequence, which lacks any known structural domains. Our hypothesis was that the presence of the half LIM domain may allow some degree of interaction of MLP-b with known MLP binding partners, while the remaining residues may enable novel functions. A series of experiments addressing this are presented below.

Proteomic identification of MLP-b by LC-MS/MS analysis

To further evaluate the expression of MLP-b at the protein level in human skeletal and cardiac muscles, LC-MS/MS analysis was performed. To distinguish between full length

MLP-a, and MLP-b, a MLP-b-specific antibody was generated that recognizes an epitope which is unique to this form of the protein (amino acids 43–56). MLP-b and full length MLP-a were isolated from striated muscle protein homogenates by immunoprecipitation with the respective antibodies, and subjected to LC-MS/MS analysis. As a positive control, purified GST-MLP-b recombinant protein was analyzed in a parallel set of reactions. Bioinformatical processing of the resulting peptide spectra versus the predicted amino acid sequence of MLP-b revealed its presence in all samples, with a confidence level >99%, and protein coverage from 98.3 to 99% (Fig. 1E). MLP-b fragments containing its unique amino acid sequence (amino acid positions 38–58), which corresponds to the alternatively spliced transcript, were observed in the GST-MLP-b and human heart immunoprecipitation samples. None of the spectra corresponding to MLP-b was assigned to any other protein when the LC-MS/MS generated spectra were tested against the *H. sapiens* UniProtKB knowledgebase or against decoy protein database, indicating the high specificity of these spectra for the MLP-b protein sequence. The combined use of a highly targeted antibody with an unbiased state-of-the-art mass spectrometry approach on human striated muscle whole protein extracts ensured high stringency, unbiased measurements and direct *in vivo* relevance, respectively.

Aberrant MLP-b expression in neuromuscular disease patients

Having identified this novel MLP isoform and confirmed its existence in striated muscle tissues by a number of different approaches, we next investigated its possible implication in muscle pathophysiology. This was based on previous reports regarding the altered expression of MLP in different neuromuscular diseases [10–12], suggesting a role for MLP in pathological phenotypes. To evaluate the potential implication of MLP-b in striated muscle disease, we analyzed the expression of MLP-a and MLP-b in skeletal muscle from patients with a variety of neuromuscular disease, including calpain-3 deficient limb girdle muscular dystrophy type 2A (LGMD2A) (n=6), Duchenne muscular dystrophy (DMD) (n=4) and dermatomyositis (DM) (n=4). Western blot analysis revealed a significant increase in MLP-b expression in all three diseases (LGDM2A: P=0.01, *t* test, two-tailed; DMD: P=0.004, *t* test, two-tailed; DM: P=0.05, *t* test, two-tailed; n=3), compared to unaffected individuals (Fig. 2A–F). While an additional lower band of unknown origin was observed in the DMD samples, quantification of MLP-b in these patients was based on the single band corresponding to the isoform reported in this manuscript to enable direct comparison of its expression levels among the different disease types examined. MLP-a levels remained unaltered in LGDM2A and DMD, but was found to be significantly increased in DM (P=0.01, *t* test, two-tailed; n=3) (Fig. 2E–F), in agreement with previous reports [12, 27–31]. The differential patterns in MLP-a and MLP-b expression across all the investigated disease types support a distinct role of these two MLP forms in striated muscle disease.

Analysis of the MLP-b:MLP-a ratio in all patient and control specimens determined a significant increase in the LGMD2A (P=0.05, *t* test, two-tailed; n=3) and DMD patients (P=0.01, *t* test, two-tailed; n=3), compared to unaffected individuals (Fig. 2G). In contrast, no significant changes were determined for the DM patients, when compared to control samples (P=0.29, *t* test, two-tailed; n=3) (Fig. 2G), suggesting disease-specific alterations in

the ratio of the two proteins and potential implications in disease pathogenesis. Collectively, the observed alterations in the expression levels of the MLP-b isoform in all three neuromuscular diseases evaluated herein, point to its association with skeletal muscle pathophysiology, thus highlighting its significance striated muscle. This prompted us to perform detailed cellular and molecular functional characterization analysis in order to decipher the molecular mechanisms associated with its significance in striated muscle.

MLP-b is expressed during early stages of myoblast differentiation

Given the established dual role of MLP in muscle differentiation as well as cytoarchitecture, we first investigated the expression pattern of MLP-b during myoblast differentiation. For this analysis, the mouse myoblast cell line C2C12 was used and the expression of full length MLP as well as MLP-b was evaluated at different stages of differentiation, both at the cDNA and protein levels. RT-PCR analysis demonstrated MLP-b expression during all time points examined (0–8 days), including myoblast and early differentiation stages (Fig. 3A). Although RT-PCR provides only semi-quantitative measure of expression levels, under these experimental conditions MLP-b isoform appears to show higher expression levels during early stages of myogenesis and modest down-regulation during late myogenic differentiation. On the contrary, full length MLP, MLP-a, was expressed during later stages of differentiation, showing highest levels of expression prior to day 8 (Fig. 3A). Similar results were obtained at the protein level, with MLP-b being detected from early stages of differentiation while MLP-a was present during later stages of myotube formation (Fig. 3B), as revealed by western blot analysis of differentiating C2C12 cells (1–8 days). Consistently with these findings, immunofluorescence studies of the same C2C12 differentiation time points showed a differential expression pattern for MLP-a and MLP-b, with the latter being detected from early differentiation stages, while MLP-a at later time points of myotube differentiation (Fig. 3C). Of note, MLP-b appeared to localize within the cytoplasm during early differentiation stages and co-distributed with the sarcomeric marker α-actinin during myotube differentiation. Collectively, these findings reveal a differential expression pattern between the novel isoform MLP-b and full length MLP, suggesting different roles in myogenesis.

MLP-b affects C2C12 differentiation to myotubes

Previous studies have demonstrated an important role for MLP in the regulation of skeletal myogenesis. To investigate the role of the novel MLP isoform in this context, C2C12 myoblasts were transfected with GFP, GFP-MLP-a, or GFP-MLP-b and allowed to differentiate (Fig. 4A). Significant changes were observed between the two MLP forms, both at the “aspect ratio” [32] and the “myotube area” [33–34]. Specifically, for the aspect ratios (defined as myotube length/diameter) of transfected C2C12 cells, the GFP- MLP-b showed the lowest values in early myotube stages, being decreased by 17% compared to GFP (P=0.10, t test, two-tailed; n=6) and by 36% compared to GFP-MLP-a (P=0.03, t test, two-tailed; n=6). Similar observations were made for late myotubes, where C2C12 cells transfected with GFP- MLP-b exhibited aspect ratios 20% lower than GFP (P=0.08, t test, two-tailed; n=6) and 37% lower than GFP-MLP-a (P=0.02, t test, two-tailed; n=6) (Fig. 4B). The total myotube area (a measure of the number and surface of myotubes per microscopic field) of cells transfected with GFP-MLP-b was also statistical significantly lower than GFP

and GFP-MLP-a transfected cells by 25% and 29% respectively (P=0.01, t test, two-tailed; n=6) (Fig. 4C). In addition to these findings, we evaluated the effect of MLP-b on myoblast fusion through direct measurement of the number of nuclei per myofiber. GFP overexpressing cells represented the control for these studies providing baseline indices of myoblast fusion which were in agreement with previous reports [35–36] (Fig. 4D). Overexpression of MLP-a was found to result in increased numbers of nuclei per myofiber (P=0.02, t test, two-tailed; n=4), while MLP-b inhibited myoblast fusion, as indicated by the reduced number of nuclei per myofiber (P=0.03, t test, two-tailed; n=5) (Fig. 4D). Collectively, these differences indicate that MLP-b overexpression serves as negative regulator of myotube differentiation, and its effect is magnified with time.

MLP-b does not associate with muscle-specific transcription factors

Overexpression of MLP has been associated with enhanced differentiation, an effect that could be attributed to its interaction with muscle transcription factors, including MyoD and Myogenin [13, 24]. To investigate whether the negative effect of the isoform on myogenesis is mediated through similar molecular mechanisms, we examined its potential interaction with the MLP-associated transcription factors MyoD and Myogenin. Recombinant proteins of full length His-MyoD and His-Myogenin were generated (Fig. 5A) and blot overlay assays with the GST-MLP-b were performed. Western blot analysis with the GST antibody determined that the isoform does not bind to MyoD or Myogenin (Fig. 5B), although it can directly bind MLP, as detected by its interaction with MBP-MLP-a recombinant protein (Fig. 5B). In a parallel set of blot overlay assays we confirmed previous reports on the direct interaction of full length MLP with MyoD and Myogenin (Fig. 5C).

Having determined that MLP-b does not associate with MyoD and Myogenin, we next investigated whether it may influence myogenesis by affecting the binding of MLP to these transcription factors. To investigate this hypothesis, we performed *in vitro* competition assays, using His-MyoD or His-Myogenin and MBP-MLP-a recombinant proteins. The interaction between these proteins was assessed in the presence or absence of GST-MLP-b. Western blot analysis using the MBP antibody did not reveal any significant changes in the interaction of His-MyoD or His-Myogenin with MBP-MLP-a in the presence of the GST-MLP-b (Fig. 5D–E). In conclusion, MLP-b does not seem to affect myocyte differentiation through the transcription machinery, but instead its effect on myotube differentiation may be mediated through different molecular mechanisms.

MLP-b localizes at the Z-disc

To determine the subcellular distribution of MLP-b in striated muscles, we performed immunofluorescence analysis in frozen sections of human quadriceps muscles with the MLP-b-specific antibody. Co-staining with MLP or α-actinin, a marker for the Z-disc, showed co-localization of MLP-b with both (Fig. 6A), thus implicating MLP-b at the level of the sarcomeric Z-discs. This finding supports a putative myofibrilar structural role of MLP-b, similarly to MLP. In addition, no perturbation in the isoform's Z-disc subcellular distribution was observed in all human neuromuscular disease patients examined (data not shown), implying the significance of the isoform at the level of the Z-disc in both physiological and pathophysiological conditions.

MLP-b associates with Z-disc proteins

Given the Z-disc localization of MLP-b, we proceeded to evaluate the molecular mechanisms associated with its functional role at this subcellular location. MLP is known to interact with a number of different structural proteins, including α-actinin and telethonin (T-cap) [6, 19] that localize at the Z-disc. Since MLP-b exhibits Z-disc distribution, we assessed whether it may also bind to these Z-disc structural components. For this analysis, we generated GST-MLP-b recombinant protein and performed pull down assays in cardiac muscle extracts. In parallel, we performed pull down assays using GST-MLP-a, which served as a positive control for these experiments (Fig. 6B). Western blot analysis of the pull down samples determined that MLP-b can bind both to α-actinin and T-cap (Fig. 6C). These findings suggest a functional role for MLP-b in the Z-disc through its interaction with structural components, with potential implications in sarcomere assembly and integrity.

MLP-b interacts with full length MLP and affects MLP regulation of CFL2-mediated F-actin depolymerization

In addition to the Z-disc structural components α-actinin and T-cap, MLP has been previously shown to associate with itself [9] and our findings indicate (Fig. 5) that it can also bind to MLP-b. In order to analyze the functional role of MLP-b at the Z-disc, we examined the minimal binding region of full length MLP protein that is involved in its interaction with MLP-b. We generated recombinant proteins of full length MBP-MLP-a, as well as different deletion constructs of MLP-a, including MBP-MLP-LIM1 (9–94 aa), MBP-MLP-LIM2 (105–188 aa) and MBP-MLP-inter-LIM (64–117 aa) (Fig. 6D), and performed blot overlay assays with the GST-MLP-b. This determined that MLP-b can bind directly to MLP-a and that this interaction is primarily occurring with the inter-LIM region of full length MLP (Fig. 6E).

As we demonstrated previously, the only known protein that binds to the inter-LIM domain is CFL2 [20], a protein involved in F-actin depolymerization. Since this interaction has direct implications on actin cytoskeleton dynamics [20], we investigated whether MLP-b can also bind directly to CFL2. Recombinant MBP-MLP and MBP-MLP-b (Fig. 6F) were assessed by blot overlay assays for their binding with GST-CFL2. Western blot analysis revealed that, in contrast to MLP, CFL2 does not bind to MLP-b (Fig. 6G). This finding suggests that MLP-b may not be implicated in regulation of cytoskeleton dynamics or that its effect on CFL2 may occur through a different mechanism.

To investigate the possibility that MLP-b may compete with CFL2 for binding to the MLP inter-LIM domain and in this way affect CFL2-dependent actin dynamics, we performed competition assays by blot overlay using His-CFL2 and MBP-MLP-a in the presence or absence of the GST-MLP-b. The MLP/CFL2 interaction remained unaffected by the presence of MLP-b, indicating that the latter does not compete with CFL2 for binding to full length MLP (Fig. 6H–I).

According to our previous observations, MLP regulates CFL2-mediated F-actin depolymerization in a MLP/CFL2 ratio sensitive manner [20]. We examine the effects of the two MLP forms on the CFL2 severing and depolymerization activities of F-actin. To this

end we performed *in vitro* pyrene-F-actin polymerization and depolymerization assays using recombinant GST-CFL2, MBP-MLP-a and/or MBP-MLP-b at suboptimal (pH 7.0 and low strength of actin polymerization buffer) and optimal conditions (pH 8.0 and when MLP is present, MLP/CFL2 ratio 2:1), respectively. We found that full length MLP, MLP-a, enhanced the CFL2 severing activity (P=0.001, t test, two-tailed; n=3) but MLP-b alone did not (Fig. 7A). However, in the presence of MLP-b, the MLP-a/CFL2 severing activity is reduced by 40% (Fig. 7B) (P=0.03, t test, two-tailed; n=3). Furthermore, MLP-b itself does not affect CFL2 depolymerization activity (Fig. 7C and 7D), but it reduces the MLP enhancement of the CFL2-mediated F-actin depolymerization by 20% (P=0.01, t test, two-tailed; n=3) (Fig. 7C and 7D). This implies that the interaction between full length MLP and MLP-b suppresses the effect of MLP on CFL2. Importantly, this finding suggests that changes in the stoichiometry of full length MLP and MLP-b may have important effects on actin dynamics during myotube differentiation and possibly under pathophysiological conditions, as observed in different types of muscular dystrophy patients.

Discussion

Accumulating evidence over the past few years has pointed to a critical role for MLP in striated muscle physiology [13, 23, 37–38]. We are now presenting a novel MLP isoform, designated as MLP-b, with distinct roles to full length MLP and differential expression in both physiological and pathological conditions. Specifically, this novel isoform serves as a negative regulator of myotube differentiation, modifies the MLP/CFL2 mediated F-actin depolymerization, and interacts with sarcomeric Z-disc proteins. Importantly, its expression is impaired in the striated muscles of neuromuscular disease patients. This evidence points to the role of MLP-b as a novel regulator of differentiation and cytoarchitecture, effects that may be mediated through its contribution to sarcomeric structural integrity and stability.

MLP contains two LIM domains and belongs to the LIM-only family, a large protein family with diverse functional roles including transcriptional regulation, cell fate determination, cell adhesion and motility, cytoskeleton organization and signal transduction [39–41]. Various isoforms have been identified for a number of LIM domain-containing proteins that are related to MLP, including SLIM1 [42], FHL1 [43–44], ALP and Enigma [45–46], however, this is the first report of a splice variant of MLP. The expression of this novel isoform was confirmed with multiple approaches at the RNA and protein level in both human and mouse skeletal and cardiac muscles. It arises from the alternative splicing of MLP exons 3 and 4, leading to changes in the reading frame and the introduction of a premature stop codon. At the protein level, MLP-b shows similarity to MLP only at its N-terminus and contains only the first half of the first LIM domain. These structural differences support a differential function in the regulation of striated muscle physiology.

To determine whether MLP-b has a significant role in striated muscle function we assessed its expression in biopsies from patients with three different neuromuscular disorders (DMD, LGMD2A or DM). Aberrations in MLP expression have been described in several different skeletal muscle diseases including facioscapulohumeral muscular dystrophy, nemaline myopathy and limb girdle muscular dystrophy type 2B [10–12] suggesting the association of MLP with diverse pathological phenotypes. In the current study, MLP-b was found

significantly overexpressed in all different human diseases examined (DMD, LGMD2A and DM), unlike MLP. This differential expression pattern suggests a distinct role of these two MLP forms in muscle pathophysiology. Since MLP-b is expressed at early stages of myocyte differentiation (as shown in C2C12 experiments), and given that the three skeletal muscle diseases present with increased skeletal muscle regeneration [47–49], it could be hypothesized that the increase in MLP-b expression may be, at least partly, a reflection of increased regeneration. Alternatively, MLP-b overexpression may represent a compensatory mechanisms aiming to reinstate structural integrity in the affected skeletal muscles. Further studies using larger number of patients will contribute towards deciphering the role of this novel MLP isoform in muscle disease.

To determine the role of MLP-b in muscle physiology and pathophysiology we used a series of complementary approaches including: (a) detection of its subcellular localization, (b) evaluation of its interaction with important sarcomeric proteins, as well as (c) its effects on MLP/CFL2-mediated actin dynamics, (d) determination of its effect on myotube differentiation following overexpression in C2C12 cells, and (e) assessment of its potential direct or indirect regulation of myogenic transcription factors. Our findings reveal that MLP-b localizes only in the cytoplasm and has an important role in regulating in structural integrity and myocyte differentiation.

Immunofluorescence analysis of skeletal muscle sections specifically demonstrated a Z-disc distribution of MLP-b. The Z-disc represents a dynamic macromolecular structure, serving as the main anchoring point for a plethora of different proteins that constitute the molecular machinery underlying muscle contraction [50–51]. In addition to the structural function that was original attributed to it, increasing evidence has revealed an emerging role of Z-disc as a nodal point and important hub of signaling networks, acting as a stretch sensor mechanism and being directly implicated in mechano-signaling and mechano-trasduction [52–56]. The involvement of MLP-b at the Z-disc was investigated by evaluating its ability to bind to components of the Z-disc. These included the Z-disc structural components α-actinin and the titin-binding protein T-cap, which have been previously shown to bind to N-terminal regions of MLP [6, 19], CFL2, a Z-disc protein involved in F-actin dynamics which we have previously identified as a binding partner of MLP [20], as well as the full length MLP, which is known to associate with itself to form oligomers [9, 21].

A direct association was observed between MLP-b and two essential structural components of the Z-disc, namely α-actinin and T-cap proteins. Importantly, previous studies have determined that dilated or hypertorphic cardiomyopathy-causing mutations of MLP (W4R and C58G) decrease its binding with α- actinin and T-cap, indicating the significance of these associations in cardiac muscle integrity [6, 19, 38]. Moreover, T-cap mutations impairing its binding to MLP have also been found to cause dilated cardiomyopathy [57]. The importance of the MLP and T-cap interaction for Z-disc stability is further supported by the selective mislocalization of T-cap, and Z-disc misalignment in the MLP −/− mouse myocardium [6]. Taken together, these findings suggest that, through its interactions with α-actinin and T-cap, MLP-b may contribute to sarcomeric structural integrity and stability. This may be mediated through its half LIM1 domain, which could serve as an anchor and adaptor domain promoting the assembly of multiprotein complexes. Given the early

expression of MLP-b during myotube differentiation that coincides with the early expression pattern of α-actinin during myofirbillogenesis that is believed to contribute to myofibril assembly [58–59], it could be hypothesized that MLP-b may play a role in early sarcomere organization. These findings point to an important role of MLP-b in muscle physiology and may at least partly explain its implication in muscle pathology.

An additional role of MLP-b is emerging at the actin cytoskeleton level, being implicated in F-actin dynamics. In particular, while full length MLP enhances CFL2 severing activity in G-actin polymerization and F-actin depolymerization in vitro, the novel isoform MLP-b diminishes both of these effects. This is likely mediated by the direct interaction of MLP-b with MLP, since the former does not affect CFL2 activities by itself and does not directly interact with CFL2. It can therefore be postulated that inhibitory effects of MLP-b on the MLP/CFL2 complex activities in F-actin dynamics are due to ratiometric changes in MLP/CFL2 interaction [20]. Structural modifications of the CFL2 catalytic domain or changes in actin filament allostery may also be involved [60], resulting in an MLP-b/MLP/CFL2 complex that is less active than the MLP/CFL2 complex.

F-actin polymerization plays an important role in muscle differentiation [61]. Based on the influence of MLP-b on in vitro F-actin dynamics, changes in MLP-b levels would be anticipated to impair this process. Indeed, overexpression of the MLP-b in C2C12 cells significantly reduced their differentiation (nuclei number per myotube, myotube area and aspect ratio), in sharp contrast to MLP, which increased C2C12 differentiation. These observations are consistent with the absence of nuclear staining or interactions with myogenic transcription factors (MyoD and myogenin) of MLP-b, as opposed to full length MLP, pointing to its indirect effect on muscle differentiation through regulation of actin dynamics.

According to our previous findings, the effect of MLP on CFL2 F-actin depolymerization activity is influenced by the stoichiometry of the two proteins, with maximal MLP/CFL2 complex activity at a protein ratio of 2:1 [20], while CFL2 alone exhibits different F-actin severing activities *in vitro* at different cofilin/actin ratios [62]. The stoichiometry of the F-actin dynamics regulatory proteins is critical in disease pathology, with alterations in the MLP/CFL2 ratio noted in the hearts of the Des−/− cardiomyopathy mouse model [20], and alterations of cofilin/actin ratio having been associated with neurodegenerative diseases, including Alzheimer's disease [63–64]. Since MLP-b can be part of the MLP/CFL2 protein complex, it could be hypothesized that alterations of the ratio between the two MLP forms may contribute to cytoskeletal integrity.

In agreement to this, our findings indicate differential changes for the MLP-b:MLP-a ratio among different muscle disease categories. In specific, even though muscular dystrophies and inflammatory myopathies present with certain clinical and histopathological similarities, they display distinct molecular profiles that are likely characteristic of their unique pathogenetic mechanisms and features [65–67]. In patients with DM, an inflammatory myopathy which is primarily caused by inflammatory response affecting intramuscular capillaries that subsequently leads to muscle damage [68], no significant changes were observed in the MLP-b:MLP-a ratio. In contrast, the ratio of the two proteins was found to

be significantly increased in patients with muscular dystrophies (LGMD2A and DMD), two distinct muscle diseases, caused by defects in the cytoskeletal proteins calpain-3 and dystrophin, respectively [69]. Deficiency of calpain-3 and dystrophin is associated with significant structural changes and defects in muscle contractility as both proteins play central role in maintenance of cytoskeletal integrity [70–72]. Given the effect of MLP-b on actin dynamics, it could be proposed that the overexpression of MLP-b, and the consequent aberrations in the stoichiometry of MLP-b:MLP-a may have a compensatory role, geared towards “rescuing” actin dynamics in the disease muscle. In support of this notion, the MLP-b:MLP-a ratio was significantly greater in the DMD patients, in comparison to LGMD2A. Since dystrophin physiologically interacts with F-actin directly and protects actin filaments against depolymerization, the increased MLP-b:MLP-a ratio would be a compensatory way to regulate actin depolymerization in its absence, as observed in DMD [73–75]. Meanwhile, calpain-3 relates to the actin cytoskeleton indirectly, through interactions with the actin-binding filamin C and titin. Therefore the effects of its mutations (as in LGMD2A) on actin depolymerization would be expected to be more modest than these of dystrophin, and the MLP-b:MLP-a compensatory mechanism activation less pronounced, as observed. In brief, based on the influence of calpain-3 and dystrophin on the actin cytoskeleton, it could be postulated that their deficiency in LGMD2A and DMD may result in increased expression of MLP-b as a means of protecting actin filaments from depolymerization and consequent cytoskeleton disruption during muscle degeneration in vivo. Targeted studies will be needed to determine the precise role of MLP-b in each pathological milieu.

In conclusion, we describe a novel isoform of MLP with a unique sequence and predicted protein structure. Our findings suggest that this isoform is a regulator of differentiation and cytoarchitecture in striated muscles, acting independently of the full length MLP protein. This discovery sheds new light to the complex role of the *CSRP3* gene in striated muscle function in health and disease, while highlighting the importance of embarking on the functional characterization of the human spliceome.

Materials and Methods

RNA isolation and RT-PCR analysis

Total RNA was isolated from human postmortem muscle tissues as previously described [20] and was used as template for cDNA preparation and PCR amplification using the CSRP3 primers 5′ GTCTTCAAGATGCCAAAC 3′ and 5′ TCTGTGCAGGATTACTTG 3′ and GAPDH primers 5′ GCCTCTACTGGCGCTGCCAAGGTG 3′ and 5′ GGTCCACCACTGACACGTTGGCAGT 3′. PCR amplification was performed using standard conditions and included 30 cycles of denaturation at 94°C for 1 minute, annealing at 54°C for 1 minute and extension at 72°C for 1 minute. The CSRP3 PCR products were cloned in the TOPO TA cloning system (Invitrogen, Carlsbad, California, USA) and sequenced (Macrogen Inc, Seoul, Korea). The sequence data from this publication have been submitted to GenBank database (**Database ID: JN898958**).

RT-PCR analysis during various stages of C2C12 myoblast differentiation (0–8 days) was performed using primers 5′ GTCTTCACCATGCCAAAC 3′ and 5′ TCTGTGGGATCACGTGG 3′ that amplify mouse Csrp3 cDNA.

Western blot analysis

Western blot analysis on whole cardiac and skeletal muscle protein extracts was performed as previously described [76], using the primary antibodies: chicken polyclonal anti-MLP (AbCam, Cambridge, UK), rabbit polyclonal anti-MLP (AbCam), or mouse monoclonal GAPDH (Sigma-Aldrich), and the secondary peroxidase-conjugated antibodies anti-chicken (AbCam), anti-rabbit (Bio-Rad Laboratories Ltd) or anti-mouse (Sigma-Aldrich) secondary antibodies.

Immunofluorescence studies

Human quadriceps muscle sections of 10 μm thickness were processed as previously described [20]. Primary antibodies included chicken anti-MLP (AbCam), mouse anti-α-actinin (Sigma-Aldrich) or rabbit polyclonal anti-MLP-b (custom generated by Sigma-Aldrich recognizing an epitope in the unique MLP-b amino acid sequence 43–56: LFPLCHLWEESGVH). Secondary antibodies included Alexa Fluor anti-rabbit 488, anti-chicken 568 or anti-mouse 633 (Invitrogen). The samples were mounted with Vectashield medium containing 4′,6-diamidino-2-phenylindole (DAPI) (Vector Laboratories, Burlingame, CA, USA) and analyzed with a Leica confocal laser scanning microscope (TCS SP5, DMI6000, inverted with the acquisition software LAS-AF).

Generation of recombinant proteins

The GST-MLP-a (1–194 aa), MBP-MLP-a (1–194 aa), MBP-MLP-LIM1 (9–94 aa), MBP-MLP-LIM2 (105–188 aa) and MBP-MLP-inter-LIM (64–117 aa) constructs have been previously described [20]. The MyoD construct was generated by PCR analysis using sense primer 5′ ATGGAGCTACTGTCGCCA 3′ and antisense primer 5′ GAGCACCTGGTATATCGG 3′, and the Myogenin construct using sense primer 5′ CCCATGGAGCTGTATGAGACA 3′ and 5′ GTTGGGCATGGTTTCATC 3′. PCR products were cloned in the EcoRI/XhoI or the EcoRI/SalI sites of the pET28 vector (Novagen, Nottingham, UK), respectively. The authenticity of all constructs was confirmed by sequence analysis (Macrogen Inc). Expression and purification of recombinant proteins was performed as previously described [77]. For blot overlay and proteomics analyses the fusion-peptides were eluted from the beads in accordance to manufacturer's instructions.

Blot overlay assays

Blot overlay assays were performed as previously described [20, 76]. Briefly, ~2.5 μg of affinity-purified His, MBP, MBP-MLP-a (1–194 aa), His-MyoD (1–320 aa) and His-Myogenin (1–224 aa) recombinant proteins were separated by SDS-PAGE and transferred to nitrocellulose membranes. Following blocking, the membranes were incubated with either 3 μg/ml GST-MLP-b fusion protein or GST-MLP-a (1–194 aa). The blots were probed with anti-GST and the immunoreactive bands were visualized using ECL reagents. In another set of experiments, affinity-purified MBP, MBP-MLP-a (1–194 aa), MBP-MLP-LIM1 (9–94

aa), MBP-MLP-LIM2 (105–188 aa) and MBP-MLP-inter-LIM (64–117 aa) recombinant proteins were allowed to interact with GST-MLP-b protein as described above.

In vitro competition assays

In vitro competition binding assays were performed by incubation of His-Myogenin protein bound to amylose resin matrices with recombinant MBP–MLP-a in 50 μL binding buffer (50 mM Tris-HCl pH 7.4, 120 mM NaCl, 10 mM NaN_3, 2 mM dithiothreitol, 0.5% Tween-20) in the presence or absence of GST-MLP-b. Following 16 h incubation at 4°C, the beads were washed three times with a solution containing 50 mM Tris-HCl pH 7.4, 120 mM NaCl, 10 mM NaN_3, 0.1% Tween-20and analyzed by western blot with rabbit anti-MBP (New England Biolabs) antibody followed by peroxidase-conjugated goat anti-rabbit (Amersham Biosciences Europe) secondary antibody. Similarly, His-MyoD recombinant protein was incubated with MBP–MLP-a or MBP–MLP-a and GST-MLP-b and analyzed as described above.

Pull down assays

Pull down assays were performed as previously described [20]. Briefly, equivalent amounts of recombinant GST, GST-MLP-a and GST-MLP-b proteins bound to glutathione-Sepharose 4B™ resin were mixed with 0.5 mg of skeletal muscle homogenates and incubated at 4°C for 16 h. The beads were washed and analyzed by western blot using α-actinin or T-cap primary antibodies (Sigma-Aldrich), and peroxidase-conjugated anti-mouse (Sigma-Aldrich) or anti-rabbit (Bio-Rad) secondary antibodies.

Cell culture

Full length human MLP and MLP-b mammalian expression constructs were generated by PCR, using the CSRP3 primers described above and the PCR products were cloned in the pEGFP vector (BD Biosciences Clontech).

C2C12 cells, a mouse myoblast cell line, (ECACC, Salisbury, UK) were maintained in Dulbecco modified Eagle medium (DMEM) supplemented with 15% fetal bovine serum (Invitrogen). Cells were transiently transfected with Dreamfect Gold (Oz Biosciences, Marseille, France), according to manufacturer's instructions. Cell differentiation and myotube formation was induced by switching to differentiation media (DMEM supplemented with 2% horse serum). Immunofluorescence analysis of endogenous proteins of C2C12 myotubes was performed as described above including 30 minute incubation with Image iT™ FX signal enhancer (Invitrogen) prior to the blocking step.

Immunoprecipitation

For the immunoprecipitation, protein homogenates from human quadriceps and cardiac muscle were pre-pre-cleared with pre-washed protein-A/G agarose beads (Roche Corp., Indianapolis, IN) overnight (o/n) on a rotary wheel at 4°C. A total of 6 μg of either rabbit polyclonal anti-MLP-b or rabbit polyclonal anti-MLP were separately conjugated to 30 μl pre-washed protein-A/G Sepharose (Amersham Biosciences) bead mixture o/n (1 μl antibody/10 μl agarose beads). Antibody-bound beads were incubated with the 0.5 mg pre-cleared protein lysates for 3 ½ h at room temperature. Immunoprecipitates were collected,

washed three times in 1X PBS and boiled for 5 min, followed by a 5 min spin at 2,000 rpm, to remove the beads.

Proteomics analysis

Protein samples, including eluted GST-MLP isoform recombinant protein as well as supernatants from immunoprecipitations performed with anti-MLP isoform or anti-MLP in either quadriceps or cardiac muscle, were precipitated with TCA procedure and washed with tetrahydrofuran. The resulting protein pellets were subjected to reduction, alkylation, and in-solution phase proteolysis with trypsin, as previously described [78]. Tryptic digests were analyzed by LC-MS^n on an Agilent 6330 iontrap system retrofitted to an 1200 nano-HPLC system equipped with a micro well plate autosampler (Agilent Technologies, Karlsruhe, Germany). The 4 most abundant multiply charged precursors above absolute intensity threshold of 10^4 were selected for MS^2 experiments using the smart fragmentation operation. All spectra obtained were processed with the ProteinPilot™ Software 4.0.8085 (Paragon algorithm, AB Sciex, Foster City, Ca), with the LTQ instrument option modified with MS tolerance value of 0.2 D and MS/MS tolerance value of 0.1 D, search effort as thorough ID, and detection protein threshold >1.3 (>95% confidence), with parallel decoy database searching and false discovery rate analysis at a threshold of 0.05.

Actin polymerization and depolymerization assays

The Actin Polymerization Biochem Kit (Cytoskeleton, Denver, CO, USA) was used to investigate actin dynamics *in vitro* on a PerkinElmer LS 55 Fluorescence spectrometer (PerkinElmer Ltd, Bucks, UK), as previously described [20]. The G-actin polymerization to F-actin was performed in suboptimal conditions pH 7.0 and actin polymerization buffer 0.25x, according to manufacturer suggestions to study CFL2 severing activity. The F-actin depolymerization was performed in the presence/absence of GST-CFL2 and MBP-MLP-a or MBP-MLP-b, at pH 8.0. The slopes of curves were calculated by curve fitting.

Human skeletal muscle biopsies

Vastus lateralis biopsies from 14 patients with three distinct neuromuscular diseases and 6 healthy individuals were snap frozen in liquid nitrogen cooled isopentane. The study design and experimental procedures were conformed to the standards set by the Declaration of Helsinki and were approved by the Ethics Committee of the Eginition Hospital of the University of Athens. All subjects provided written informed consent.

Diagnosis of the six patients LGMD2A, aged 16–40 years, was based on reduced calpain-3 expression in western blot analysis and mutations in the calpain-3 gene detected by direct sequencing. All patients presented with mild muscular weakness (manual muscle testing scores 3–5/5). Blood CPK values ranged between 1000–5000 iu/ml. Histochemical analysis of their muscle biopsies revealed mild necrosis, phagocytosis, and rarely fibre regeneration.

Four patients with Duchenne muscular dystrophy (DMD), aged 4–9 years, were diagnosed based on the clinical features as well as the complete lack of dystrophin expression in immunohistochemical analysis. Patients reported with muscular weakness, difficulty in running and climbing stairs, and blood CPK between 10400–25000 iu/ml.

The four dermatomyositis (DM) patients, 19–45 years old, presented with muscular weakness (manual muscle testing scores 3/5) and various blood CPK values (100–20000 iu/ml). Histological analysis of their muscle biopsies revealed increased infiltration of inflammatory cells, moderate necrosis, phagocytosis, and regeneration.

The postmortem human cardiac, quadriceps, deltoid, diaphragm and sternocleidomastoid muscle specimens which were used for the identification of the MLP isoform, were obtained from the Department of Forensics and Toxicology, Medical School, National and Kapodistrian University of Athens as described in [20].

Acknowledgments

We are grateful to Professor Chara Spiliopoulou and Dr Stavroula Papadodima for providing the post-mortem muscle specimens and the Biological Imaging Unit at Biomedical Research Foundation for assistance with confocal imaging.

This study was supported by the Hellenic Cardiological Society. EV, DAA, EGK and DS are funded by the European Community's Seventh Framework Program FP7/2007-2013 under grant agreement no HEALTH-F2-2009-241526, EUTrigTreat.

Abbreviations

MLP	Muscle Lim Protein
CFL2	cofilin-2
CSRP3	cysteine and glycine-rich protein 3
GST	Glutathione S-transferase
MBP	maltose binding protein
His	histidine
GFP	green fluorescent protein
LC-MS/MS	Liquid chromatography-mass spectrometry/mass spectrometry
LGMD2A	limb girdle muscular dystrophy type 2A
DMD	Duchenne muscular dystrophy
DM	dermatomyositis

References

1. Arber S, Halder G, Caroni P. Muscle LIM protein, a novel essential regulator of myogenesis, promotes myogenic differentiation. Cell. 1994; 79:221–231. [PubMed: 7954791]
2. Bos JM, Poley RN, Ny M, Tester DJ, Xu X, Vatta M, Towbin JA, Gersh BJ, Ommen SR, Ackerman MJ. Genotype-phenotype relationships involving hypertrophic cardiomyopathy-associated mutations in titin, muscle LIM protein, and telethonin. Mol Genet Metab. 2006; 88:78–85. [PubMed: 16352453]
3. Geier C, Gehmlich K, Ehler E, Hassfeld S, Perrot A, Hayess K, Cardim N, Wenzel K, Erdmann B, Krackhardt F, et al. Beyond the sarcomere: CSRP3 mutations cause hypertrophic cardiomyopathy. Hum Mol Genet. 2008; 17:2753–2765. [PubMed: 18505755]

4. Geier C, Perrot A, Ozcelik C, Binner P, Counsell D, Hoffmann K, Pilz B, Martiniak Y, Gehmlich K, van der Ven PF, et al. Mutations in the human muscle LIM protein gene in families with hypertrophic cardiomyopathy. Circulation. 2003; 107:1390–1395. [PubMed: 12642359]
5. Hershberger RE, Parks SB, Kushner JD, Li D, Ludwigsen S, Jakobs P, Nauman D, Burgess D, Partain J, Litt M. Coding sequence mutations identified in MYH7, TNNT2, SCN5A, CSRP3, LBD3, and TCAP from 313 patients with familial or idiopathic dilated cardiomyopathy. Clin Transl Sci. 2008; 1:21–26. [PubMed: 19412328]
6. Knoll R, Hoshijima M, Hoffman HM, Person V, Lorenzen-Schmidt I, Bang ML, Hayashi T, Shiga N, Yasukawa H, Schaper W, et al. The cardiac mechanical stretch sensor machinery involves a Z disc complex that is defective in a subset of human dilated cardiomyopathy. Cell. 2002; 111:943–955. [PubMed: 12507422]
7. Mohapatra B, Jimenez S, Lin JH, Bowles KR, Coveler KJ, Marx JG, Chrisco MA, Murphy RT, Lurie PR, Schwartz RJ, et al. Mutations in the muscle LIM protein and alpha-actinin-2 genes in dilated cardiomyopathy and endocardial fibroelastosis. Mol Genet Metab. 2003; 80:207–215. [PubMed: 14567970]
8. Moller DV, Andersen PS, Hedley P, Ersboll MK, Bundgaard H, Moolman-Smook J, Christiansen M, Kober L. The role of sarcomere gene mutations in patients with idiopathic dilated cardiomyopathy. Eur J Hum Genet. 2009; 17:1241–1249. [PubMed: 19293840]
9. Zolk O, Caroni P, Bohm M. Decreased expression of the cardiac LIM domain protein MLP in chronic human heart failure. Circulation. 2000; 101:2674–2677. [PubMed: 10851202]
10. Sanoudou D, Corbett MA, Han M, Ghoddusi M, Nguyen MA, Vlahovich N, Hardeman EC, Beggs AH. Skeletal muscle repair in a mouse model of nemaline myopathy. Hum Mol Genet. 2006; 15:2603–2612. [PubMed: 16877500]
11. von der Hagen M, Laval SH, Cree LM, Haldane F, Pocock M, Wappler I, Peters H, Reitsamer HA, Hoger H, Wiedner M, et al. The differential gene expression profiles of proximal and distal muscle groups are altered in pre-pathological dysferlin-deficient mice. Neuromuscul Disord. 2005; 15:863–877. [PubMed: 16288871]
12. Winokur ST, Chen YW, Masny PS, Martin JH, Ehmsen JT, Tapscott SJ, van der Maarel SM, Hayashi Y, Flanigan KM. Expression profiling of FSHD muscle supports a defect in specific stages of myogenic differentiation. Hum Mol Genet. 2003; 12:2895–2907. [PubMed: 14519683]
13. Arber S, Hunter JJ, Ross J Jr, Hongo M, Sansig G, Borg J, Perriard JC, Chien KR, Caroni P. MLP-deficient mice exhibit a disruption of cardiac cytoarchitectural organization, dilated cardiomyopathy, and heart failure. Cell. 1997; 88:393–403. [PubMed: 9039266]
14. Knoll R, Hoshijima M, Chien KR. Muscle LIM protein in heart failure. Exp Clin Cardiol. 2002; 7:104–105. [PubMed: 19649232]
15. Schmeichel KL, Beckerle MC. The LIM domain is a modular protein-binding interface. Cell. 1994; 79:211–219. [PubMed: 7954790]
16. Weiskirchen R, Gunther K. The CRP/MLP/TLP family of LIM domain proteins: acting by connecting. Bioessays. 2003; 25:152–162. [PubMed: 12539241]
17. Ehler E, Horowits R, Zuppinger C, Price RL, Perriard E, Leu M, Caroni P, Sussman M, Eppenberger HM, Perriard JC. Alterations at the intercalated disk associated with the absence of muscle LIM protein. J Cell Biol. 2001; 153:763–772. [PubMed: 11352937]
18. Flick MJ, Konieczny SF. The muscle regulatory and structural protein MLP is a cytoskeletal binding partner of betaI-spectrin. J Cell Sci. 2000; 113 (Pt 9):1553–1564. [PubMed: 10751147]
19. Gehmlich K, Geier C, Osterziel KJ, Van der Ven PF, Furst DO. Decreased interactions of mutant muscle LIM protein (MLP) with N-RAP and alpha-actinin and their implication for hypertrophic cardiomyopathy. Cell Tissue Res. 2004; 317:129–136. [PubMed: 15205937]
20. Papalouka V, Arvanitis DA, Vafiadaki E, Mavroidis M, Papadodima SA, Spiliopoulou CA, Kremastinos DT, Kranias EG, Sanoudou D. Muscle LIM protein interacts with cofilin 2 and regulates F-actin dynamics in cardiac and skeletal muscle. Mol Cell Biol. 2009; 29:6046–6058. [PubMed: 19752190]
21. Arber S, Caroni P. Specificity of single LIM motifs in targeting and LIM/LIM interactions in situ. Genes Dev. 1996; 10:289–300. [PubMed: 8595880]

22. Stronach BE, Renfranz PJ, Lilly B, Beckerle MC. Muscle LIM proteins are associated with muscle sarcomeres and require dMEF2 for their expression during Drosophila myogenesis. Mol Biol Cell. 1999; 10:2329–2342. [PubMed: 10397768]

23. Buyandelger B, Ng KE, Miocic S, Piotrowska I, Gunkel S, Ku CH, Knoll R. MLP (muscle LIM protein) as a stress sensor in the heart. Pflugers Arch. 2011; 462:135–142. [PubMed: 21484537]

24. Kong Y, Flick MJ, Kudla AJ, Konieczny SF. Muscle LIM protein promotes myogenesis by enhancing the activity of MyoD. Mol Cell Biol. 1997; 17:4750–4760. [PubMed: 9234731]

25. Felkin LE, Narita T, Germack R, Shintani Y, Takahashi K, Sarathchandra P, Lopez-Olaneta MM, Gomez-Salinero JM, Suzuki K, Barton PJ, et al. Calcineurin splicing variant calcineurin Abeta1 improves cardiac function after myocardial infarction without inducing hypertrophy. Circulation. 2011; 123:2838–2847. [PubMed: 21632490]

26. Guo W, Schafer S, Greaser ML, Radke MH, Liss M, Govindarajan T, Maatz H, Schulz H, Li S, Parrish AM, et al. RBM20, a gene for hereditary cardiomyopathy, regulates titin splicing. Nat Med. 2012; 18:766–773. [PubMed: 22466703]

27. Chen YW, Zhao P, Borup R, Hoffman EP. Expression profiling in the muscular dystrophies: identification of novel aspects of molecular pathophysiology. J Cell Biol. 2000; 151:1321–1336. [PubMed: 11121445]

28. Haslett JN, Sanoudou D, Kho AT, Bennett RR, Greenberg SA, Kohane IS, Beggs AH, Kunkel LM. Gene expression comparison of biopsies from Duchenne muscular dystrophy (DMD) and normal skeletal muscle. Proc Natl Acad Sci U S A. 2002; 99:15000–15005. [PubMed: 12415109]

29. Haslett JN, Sanoudou D, Kho AT, Han M, Bennett RR, Kohane IS, Beggs AH, Kunkel LM. Gene expression profiling of Duchenne muscular dystrophy skeletal muscle. Neurogenetics. 2003; 4:163–171. [PubMed: 12698323]

30. Pescatori M, Broccolini A, Minetti C, Bertini E, Bruno C, D'Amico A, Bernardini C, Mirabella M, Silvestri G, Giglio V, et al. Gene expression profiling in the early phases of DMD: a constant molecular signature characterizes DMD muscle from early postnatal life throughout disease progression. FASEB J. 2007; 21:1210–1226. [PubMed: 17264171]

31. Saenz A, Azpitarte M, Armananzas R, Leturcq F, Alzualde A, Inza I, Garcia-Bragado F, De la Herran G, Corcuera J, Cabello A, et al. Gene expression profiling in limb-girdle muscular dystrophy 2A. PLoS One. 2008; 3:e3750. [PubMed: 19015733]

32. Ren K, Crouzier T, Roy C, Picart C. Polyelectrolyte multilayer films of controlled stiffness modulate myoblast cells differentiation. Adv Funct Mater. 2008; 18:1378–1389. [PubMed: 18841249]

33. Charrasse S, Comunale F, Grumbach Y, Poulat F, Blangy A, Gauthier-Rouviere C. RhoA GTPase regulates M-cadherin activity and myoblast fusion. Mol Biol Cell. 2006; 17:749–759. [PubMed: 16291866]

34. Lecomte V, Meugnier E, Euthine V, Durand C, Freyssenet D, Nemoz G, Rome S, Vidal H, Lefai E. A new role for sterol regulatory element binding protein 1 transcription factors in the regulation of muscle mass and muscle cell differentiation. Mol Cell Biol. 2010; 30:1182–1198. [PubMed: 20028734]

35. Favreau C, Higuet D, Courvalin JC, Buendia B. Expression of a mutant lamin A that causes Emery-Dreifuss muscular dystrophy inhibits in vitro differentiation of C2C12 myoblasts. Mol Cell Biol. 2004; 24:1481–1492. [PubMed: 14749366]

36. Shafey D, Cote PD, Kothary R. Hypomorphic Smn knockdown C2C12 myoblasts reveal intrinsic defects in myoblast fusion and myotube morphology. Exp Cell Res. 2005; 311:49–61. [PubMed: 16219305]

37. Barash IA, Mathew L, Lahey M, Greaser ML, Lieber RL. Muscle LIM protein plays both structural and functional roles in skeletal muscle. Am J Physiol Cell Physiol. 2005; 289:C1312–1320. [PubMed: 16093282]

38. Knoll R, Kostin S, Klede S, Savvatis K, Klinge L, Stehle I, Gunkel S, Kotter S, Babicz K, Sohns M, et al. A common MLP (muscle LIM protein) variant is associated with cardiomyopathy. Circ Res. 2010; 106:695–704. [PubMed: 20044516]

39. Kadrmas JL, Beckerle MC. The LIM domain: from the cytoskeleton to the nucleus. Nat Rev Mol Cell Biol. 2004; 5:920–931. [PubMed: 15520811]

40. Schmeichel KL, Beckerle MC. Molecular dissection of a LIM domain. Mol Biol Cell. 1997; 8:219–230. [PubMed: 9190203]
41. Zheng Q, Zhao Y. The diverse biofunctions of LIM domain proteins: determined by subcellular localization and protein-protein interaction. Biol Cell. 2007; 99:489–502. [PubMed: 17696879]
42. Brown S, McGrath MJ, Ooms LM, Gurung R, Maimone MM, Mitchell CA. Characterization of two isoforms of the skeletal muscle LIM protein 1, SLIM1. Localization of SLIM1 at focal adhesions and the isoform slimmer in the nucleus of myoblasts and cytoplasm of myotubes suggests distinct roles in the cytoskeleton and in nuclear-cytoplasmic communication. J Biol Chem. 1999; 274:27083–27091. [PubMed: 10480922]
43. Lee SM, Li HY, Ng EK, Or SM, Chan KK, Kotaka M, Chim SS, Tsui SK, Waye MM, Fung KP, et al. Characterization of a brain-specific nuclear LIM domain protein (FHL1B) which is an alternatively spliced variant of FHL1. Gene. 1999; 237:253–263. [PubMed: 10524257]
44. Ng EK, Lee SM, Li HY, Ngai SM, Tsui SK, Waye MM, Lee CY, Fung KP. Characterization of tissue-specific LIM domain protein (FHL1C) which is an alternatively spliced isoform of a human LIM-only protein (FHL1). J Cell Biochem. 2001; 82:1–10. [PubMed: 11400158]
45. Yamazaki T, Walchli S, Fujita T, Ryser S, Hoshijima M, Schlegel W, Kuroda S, Maturana AD. Splice variants of enigma homolog, differentially expressed during heart development, promote or prevent hypertrophy. Cardiovasc Res. 2010; 86:374–382. [PubMed: 20097676]
46. Zheng M, Cheng H, Banerjee I, Chen J. ALP/Enigma PDZ-LIM domain proteins in the heart. J Mol Cell Biol. 2010; 2:96–102. [PubMed: 20042479]
47. Dimachkie MM. Idiopathic inflammatory myopathies. J Neuroimmunol. 2011; 231:32–42. [PubMed: 21093064]
48. Loell I, Lundberg IE. Can muscle regeneration fail in chronic inflammation: a weakness in inflammatory myopathies? J Intern Med. 2011; 269:243–257. [PubMed: 21205023]
49. Wallace GQ, McNally EM. Mechanisms of muscle degeneration, regeneration, and repair in the muscular dystrophies. Annu Rev Physiol. 2009; 71:37–57. [PubMed: 18808326]
50. Faulkner G, Lanfranchi G, Valle G. Telethonin and other new proteins of the Z-disc of skeletal muscle. IUBMB Life. 2001; 51:275–282. [PubMed: 11699871]
51. Frank D, Kuhn C, Katus HA, Frey N. The sarcomeric Z-disc: a nodal point in signalling and disease. J Mol Med (Berl). 2006; 84:446–468. [PubMed: 16416311]
52. Buyandelger B, Ng KE, Miocic S, Gunkel S, Piotrowska I, Ku C, Knoll R. Genetics of mechanosensation in the heart. J Cardiovasc Transl Res. 2011; 4:238–244. [PubMed: 21360311]
53. Frank D, Frey N. Cardiac Z-disc signaling network. J Biol Chem. 2011; 286:9897–9904. [PubMed: 21257757]
54. Gautel M. The sarcomeric cytoskeleton: who picks up the strain? Curr Opin Cell Biol. 2011; 23:39–46. [PubMed: 21190822]
55. Luther PK. The vertebrate muscle Z-disc: sarcomere anchor for structure and signalling. J Muscle Res Cell Motil. 2009; 30:171–185. [PubMed: 19830582]
56. Pyle WG, Solaro RJ. At the crossroads of myocardial signaling: the role of Z-discs in intracellular signaling and cardiac function. Circ Res. 2004; 94:296–305. [PubMed: 14976140]
57. Hayashi T, Arimura T, Itoh-Satoh M, Ueda K, Hohda S, Inagaki N, Takahashi M, Hori H, Yasunami M, Nishi H, et al. Tcap gene mutations in hypertrophic cardiomyopathy and dilated cardiomyopathy. J Am Coll Cardiol. 2004; 44:2192–2201. [PubMed: 15582318]
58. Ehler E, Gautel M. The sarcomere and sarcomerogenesis. Adv Exp Med Biol. 2008; 642:1–14. [PubMed: 19181089]
59. Kontrogianni-Konstantopoulos A, Catino DH, Strong JC, Bloch RJ. De novo myofibrillogenesis in C2C12 cells: evidence for the independent assembly of M bands and Z disks. Am J Physiol Cell Physiol. 2006; 290:C626–637. [PubMed: 16207790]
60. Pfaendtner J, De La Cruz EM, Voth GA. Actin filament remodeling by actin depolymerization factor/cofilin. Proc Natl Acad Sci U S A. 2010; 107:7299–7304. [PubMed: 20368459]
61. Kihara T, Shinohara S, Fujikawa R, Sugimoto Y, Murata M, Miyake J. Regulation of cysteine-rich protein 2 localization by the development of actin fibers during smooth muscle cell differentiation. Biochem Biophys Res Commun. 2011; 411:96–101. [PubMed: 21718689]

62. Andrianantoandro E, Pollard TD. Mechanism of actin filament turnover by severing and nucleation at different concentrations of ADF/cofilin. Mol Cell. 2006; 24:13–23. [PubMed: 17018289]

63. Bamburg JR, Bernstein BW, Davis RC, Flynn KC, Goldsbury C, Jensen JR, Maloney MT, Marsden IT, Minamide LS, Pak CW, et al. ADF/Cofilin-actin rods in neurodegenerative diseases. Curr Alzheimer Res. 2010; 7:241–250. [PubMed: 20088812]

64. Bernstein BW, Bamburg JR. ADF/cofilin: a functional node in cell biology. Trends Cell Biol. 2010; 20:187–195. [PubMed: 20133134]

65. Eisenberg I, Eran A, Nishino I, Moggio M, Lamperti C, Amato AA, Lidov HG, Kang PB, North KN, Mitrani-Rosenbaum S, et al. Distinctive patterns of microRNA expression in primary muscular disorders. Proc Natl Acad Sci U S A. 2007; 104:17016–17021. [PubMed: 17942673]

66. Greenberg SA, Sanoudou D, Haslett JN, Kohane IS, Kunkel LM, Beggs AH, Amato AA. Molecular profiles of inflammatory myopathies. Neurology. 2002; 59:1170–1182. [PubMed: 12391344]

67. Hoffman EP, Rao D, Pachman LM. Clarifying the boundaries between the inflammatory and dystrophic myopathies: insights from molecular diagnostics and microarrays. Rheum Dis Clin North Am. 2002; 28:743–757. [PubMed: 12506770]

68. Dalakas MC. Pathogenesis and therapies of immune-mediated myopathies. Autoimmun Rev. 2012; 11:203–206. [PubMed: 21619945]

69. McNally EM, Pytel P. Muscle diseases: the muscular dystrophies. Annu Rev Pathol. 2007; 2:87–109.10.1146/annurev.pathol.2.010506.091936 [PubMed: 18039094]

70. Deconinck N, Dan B. Pathophysiology of duchenne muscular dystrophy: current hypotheses. Pediatr Neurol. 2007; 36:1–7. [PubMed: 17162189]

71. Duguez S, Bartoli M, Richard I. Calpain 3: a key regulator of the sarcomere? FEBS J. 2006; 273:3427–3436. [PubMed: 16884488]

72. Laval SH, Bushby KM. Limb-girdle muscular dystrophies--from genetics to molecular pathology. Neuropathol Appl Neurobiol. 2004; 30:91–105. [PubMed: 15043707]

73. Henderson DM, Lin AY, Thomas DD, Ervasti JM. The carboxy-terminal third of dystrophin enhances actin binding activity. J Mol Biol. 2012; 416:414–424. [PubMed: 22226838]

74. Prochniewicz E, Henderson D, Ervasti JM, Thomas DD. Dystrophin and utrophin have distinct effects on the structural dynamics of actin. Proc Natl Acad Sci U S A. 2009; 106:7822–7827. [PubMed: 19416869]

75. Rybakova IN, Humston JL, Sonnemann KJ, Ervasti JM. Dystrophin and utrophin bind actin through distinct modes of contact. J Biol Chem. 2006; 281:9996–10001. [PubMed: 16478721]

76. Arvanitis DA, Vafiadaki E, Fan GC, Mitton BA, Gregory KN, Del Monte F, Kontrogianni-Konstantopoulos A, Sanoudou D, Kranias EG. Histidine-rich Ca-binding protein interacts with sarcoplasmic reticulum Ca-ATPase. Am J Physiol Heart Circ Physiol. 2007; 293:H1581–1589. [PubMed: 17526652]

77. Vafiadaki E, Sanoudou D, Arvanitis DA, Catino DH, Kranias EG, Kontrogianni-Konstantopoulos A. Phospholamban interacts with HAX-1, a mitochondrial protein with anti-apoptotic function. J Mol Biol. 2007; 367:65–79. [PubMed: 17241641]

78. Emmanouilidou E, Melachroinou K, Roumeliotis T, Garbis SD, Ntzouni M, Margaritis LH, Stefanis L, Vekrellis K. Cell-produced alpha-synuclein is secreted in a calcium-dependent manner by exosomes and impacts neuronal survival. J Neurosci. 2010; 30:6838–6851. [PubMed: 20484626]

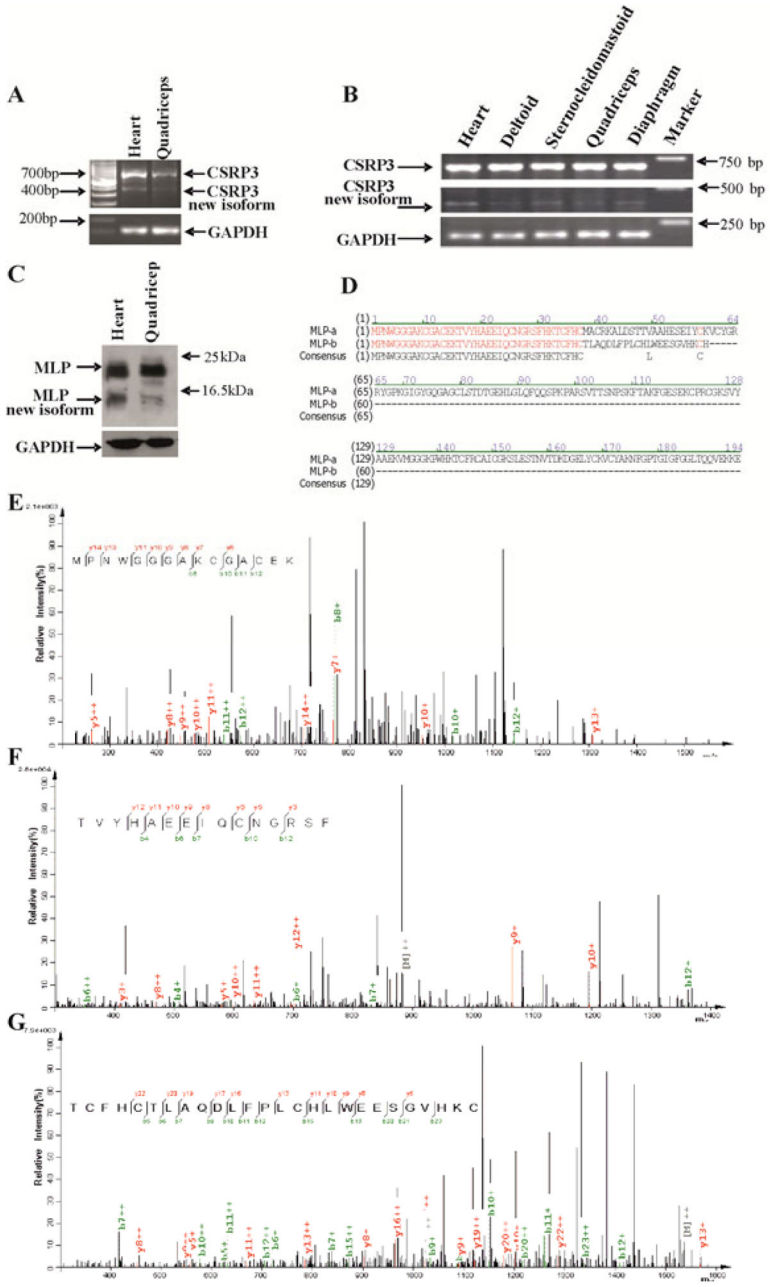

Fig. 1. Identification of a novel CSRP3 isoform in striated muscles

(A) RT-PCR analysis of CSRP3 in cardiac and skeletal muscle cDNA generated, in addition to the full length CSRP3 cDNA, a shorter product of ~400bp that represents a novel putative CSRP3 isoform. (B) Expression of this new isoform was also detected in different skeletal muscle tissues, indicating a role in striated muscles. (C) Western blot analysis of cardiac and skeletal muscle extracts confirmed the expression of the novel MLP isoform at the protein level. (D) Alignment of predicted amino acid sequence of the novel MLP isoform, MLP-b, against full length MLP, MLP-a, reveals a consensus of 37 amino acids (shown in red), including the first half of LIM1 domain, and 22 unique amino acids for the new MLP isoform. (E) Representative examples of peptide identification of MLP-b from human

striated muscle after immunoprecipitation and LC-MS/MS proteomic analysis. Amino acid residues 1–15 were found using anti-MLP-b from human quadriceps muscle (confidence score=0.96), (F) amino acid residues 16–30 were found using anti-MLP-b from human heart muscle (confidence score=0.99), and (G) amino acid residues 33–58 were found using anti-MLP from human heart (confidence score=0.98). The latest contain the unique amino acid sequence (amino acid positions 38–58) of the new isoform. Amino acid residues 31–32 were not observed in any of the spectra obtained.

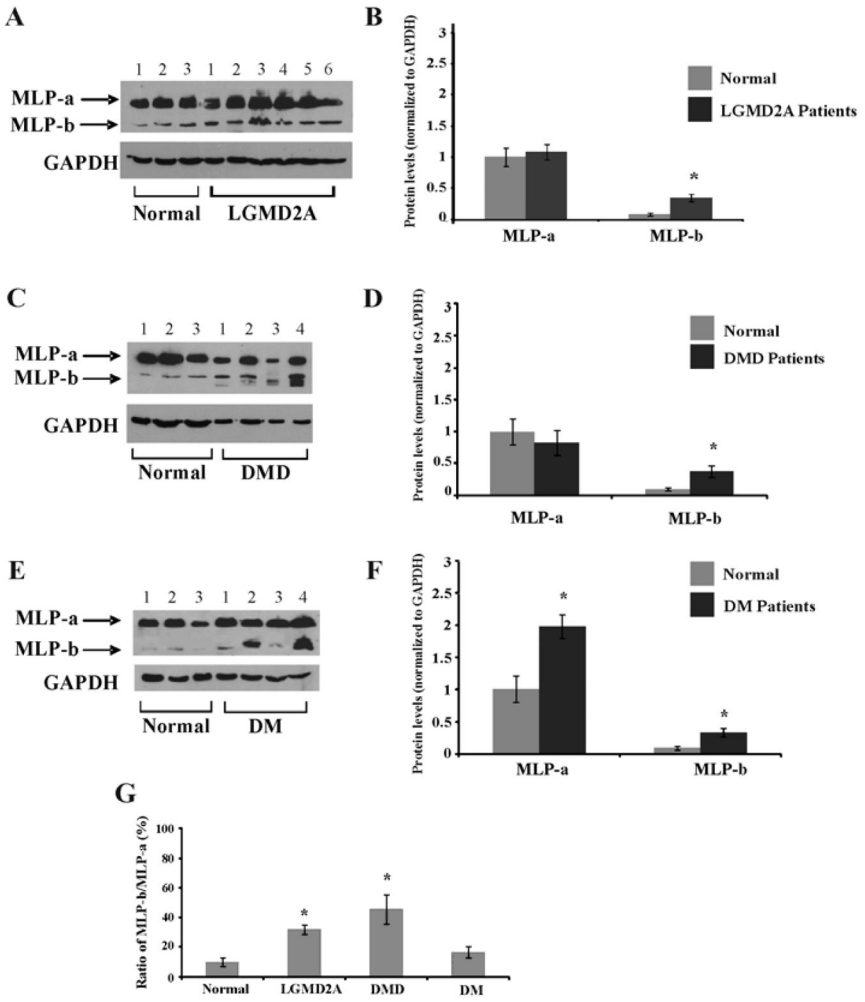

Fig. 2. Aberrant expression of full length MLP and MLP-b in human skeletal myopathy patients

Western blot analysis of (A) normal or (B) six human LGMD2A patients determined alterations in the expression levels of MLP-b. (C) Quantification of protein levels determined a significant increase of the isoform in LGDM2A patients, compared to normal samples (P=0.01, t-test, two-tailed; n=4). (D–E) Western blot analysis of four human DMD patients determined no changes in full length MLP, MLP-a, expression but a significant increase of MLP-b in DMD patients, compared to normal samples (P=0.004, t-test, two-tailed; n=4). (F–G) Analysis of four human DM patients determined a significant increase in both full length MLP (P=0.009, t-test, two-tailed; n=4) and MLP-b (P=0.05, t-test, two-tailed; n=4) protein levels in DM patients, compared to normal samples. (H) Examination of the MLP-b: MLP-a protein ratio among normals and the different groups of skeletal myopathies determined a significant increase in the LGMD2A (P=0.05, t-test, two-tailed; n=4) and DMD patients (P=0.01, t-test, two-tailed; n=4). Data are mean ± SEM.

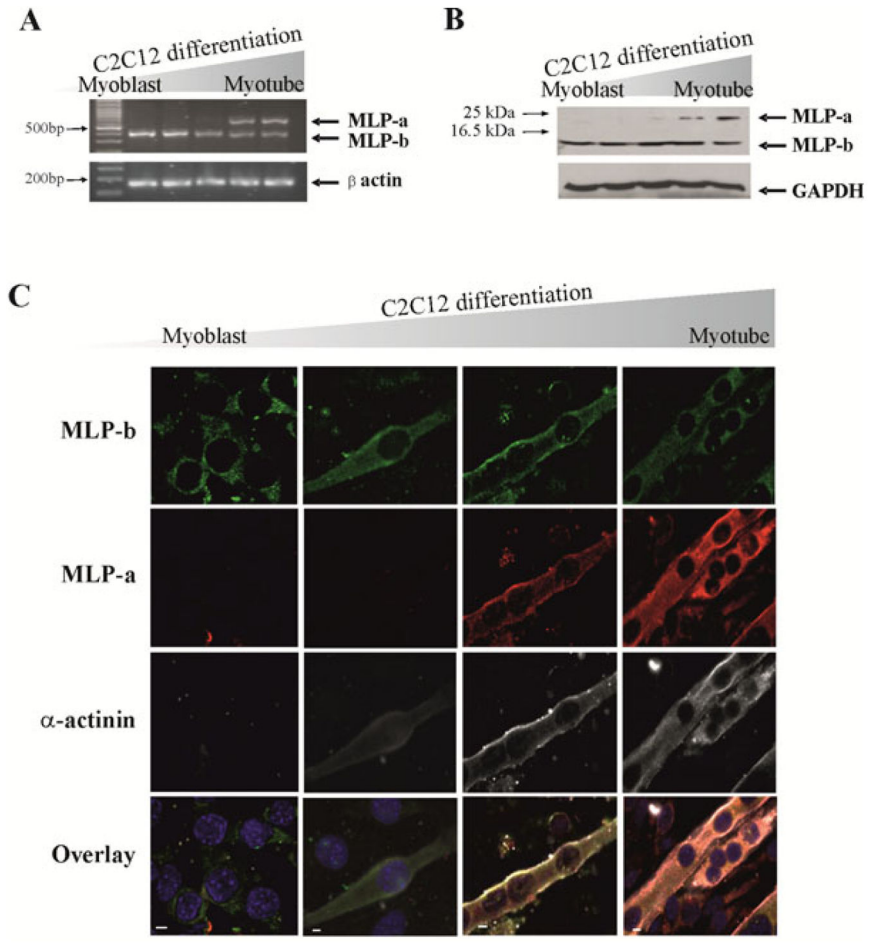

Fig. 3. MLP-b is expressed during early stages of myotube differentiation

(A) RT-PCR analysis of full length MLP, MLP-a, and MLP-b during C2C12 differentiation (0–8 days) determined that MLP-b is expressed from early stages of myotube differentiation. (B) Western blot analysis of C2C12 cell lysates during different stages of myotube differentiation (0–8 days) confirmed the expression of MLP-b during early stages of myotube differentiation. (C) Immunofluorescence analysis of C2C12 myotubes obtained during different stages of differentiation (1–8 days) was performed for MLP-a and MLP-b, as well as the Z-disc marker α-actinin. Scale bar, 5μm.

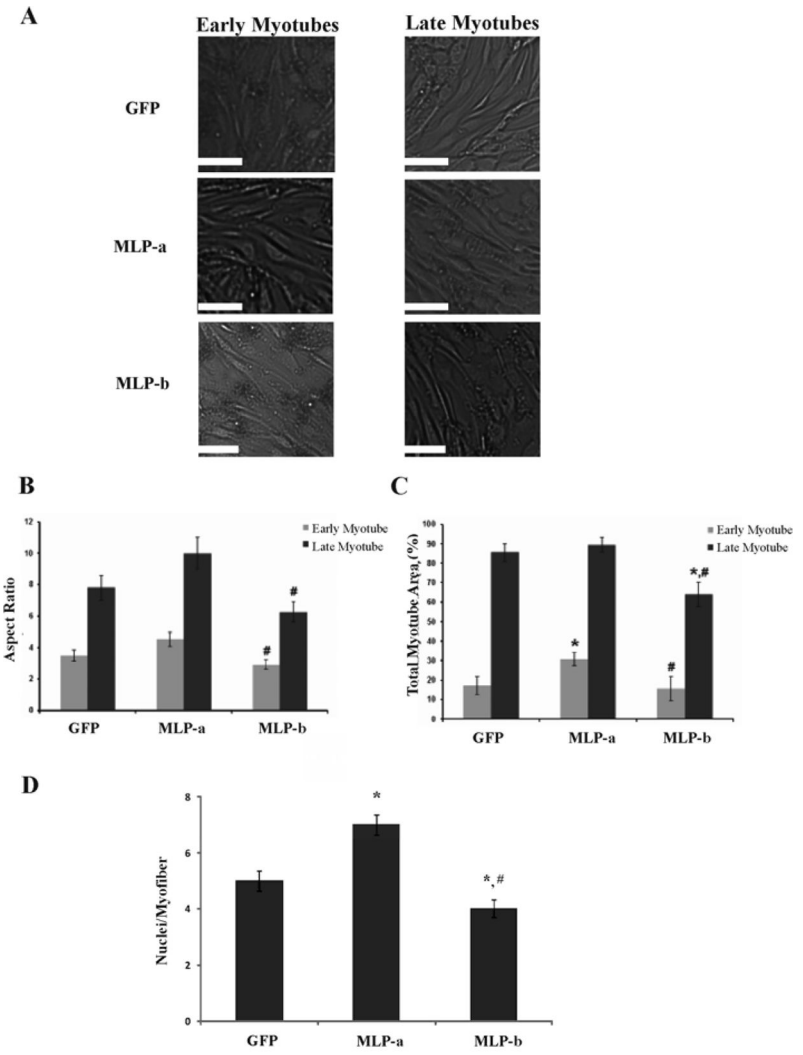

Fig. 4. MLP-b overexpression reduces C2C12 differentiation

(A) Representative images of C2C12 cells of early myotube (left panel) and late myotube stages (right), transfected with GFP, GFP-MLP-a or GFP-MLP-b. The scale bar (white) represents 100 μm. (B) Graphical representation of the aspect ratio (as length/diameter) of early (light gray) and late myotubes (dark gray), transfected with GFP, GFP-MLP-a, and GFP-MLP-b. The aspect ratio of MLP-b is statistically significantly lower than full length MLP at early myotubes (#, MLP-b vs MLP-a, P=0.03, t test, two-tailed, n=6) and late myotubes (#, MLP-b vs MLP-a, P=0.02, t test, two-tailed, n=6). (C) Graphical representation of the total myotube area (as percent of the microscopic field area covered by myotubes) at early myotube (light gray) and late myotube stages (dark gray), from C2C12 transfected with GFP, GFP-MLP-a and GFP-MLP-b. Overexpression of full length MLP, MLP-a, enhances C2C12 differentiation of early myotubes compared to GFP (* MLP-a vs GFP, P=0.03, t test, two-tailed; n=6) but MLP-b overexpression exhibits lower degree of C2C12 differentiation at late myotube stages (#, MLP-b vs MLP-a, P=0.02, t test, two-tailed, n=6; * MLP-b vs GFP, P=0.01, t test, two-tailed; n=6). (D) Measurement of nuclei number per myofiber in late myotubes of C2C12 transfected with GFP, GFP-MLP-a and

GFP-MLP-b. Overexpression of full length MLP-a increases the number of nuclei per myofiber (* MLP-a vs GFP, P=0.02, t test, two-tailed; n=4), while overexpression of MLP-b reduced number of nuclei per myofiber (* MLP-b vs GFP, P=0.03, t test, two-tailed; n=5; # MLP-b vs MLP-a, P=0.02, t test, two-tailed, n=4). Data are mean ± SEM.

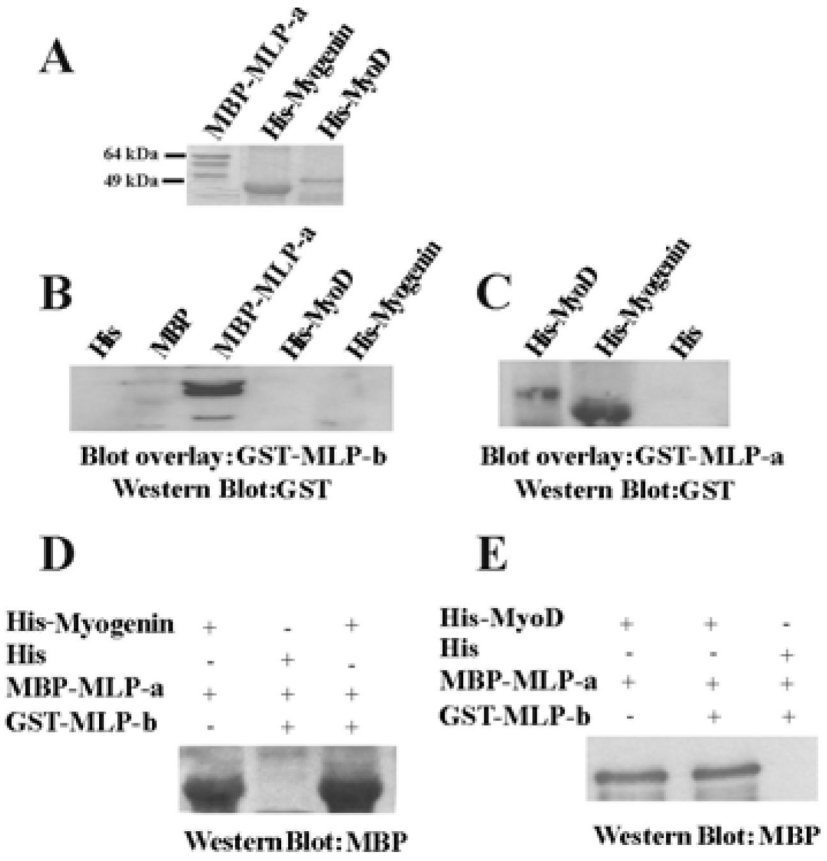

Fig. 5. MLP-b does not associate with muscle-specific transcription factors

(A) Coomassie staining of purified recombinant proteins generated for full length MBP-MLP-a, His-MyoD and His-Myogenin. (B) Blot overlay assays were performed on His-MyoD, His-Myogenin and MBP-MLP-a recombinant proteins using GST-MLP-b. Western blot analysis with GST antibody determined that MLP-b does not bind to the transcription factors but it can interact with MLP-a. (C) Blot overlay assays on His-MyoD and His-Myogenin recombinant proteins using GST-MLP-a protein confirmed its interaction with these transcription factors. *In vitro* competition assays using (D) His-Myogenin, MBP-MLP-a and GST-MLP-b or (E) His-MyoD, MBP-MLP and GST-MLP-b determined that MLP-b does not influence the association of full length MLP with the transcription factors.

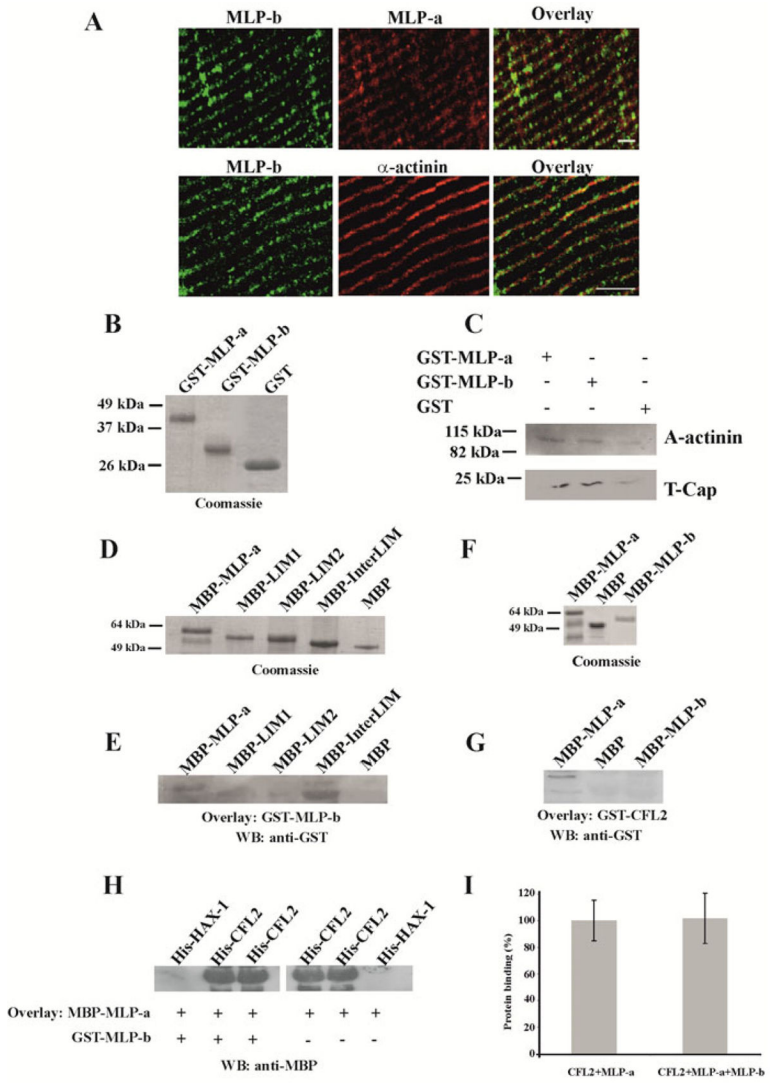

Fig. 6. MLP-b is localized at the Z-disc in skeletal muscle and interacts with the inter-LIM region of MLP, α-actinin and T-Cap

(A) Immunofluorescence analysis in skeletal muscle sections determined a Z-disc localization for MLP-b, as indicated by its co-distribution with full length MLP, MLP- a, and its co-localization with the Z-disc marker protein, α-actinin. Scale bar, 5μm. (B) SDS-PAGE analysis and Coomassie staining of purified GST-MLP-a, GST-MLP-b and GST recombinant proteins. (C) Pull down assays in cardiac homogenates determined that, similar to full length MLP, MLP-b interacts with α-actinin and T-cap proteins. (D) Coomassie staining of purified recombinant proteins generated for full length MBP-MLP-a as well as different deletion constructs. (E) Blot overlay assays were performed on MLP deletion constructs to determine the minimal binding region of MLP-b. Western blot analysis with GST antibody determined that MLP-b binds to inter-LIM region of full length MLP. (F) Coomassie staining of purified MBP-MLP-a, MBP and MBP-MLP-b recombinant proteins. (G) In contrast to full length MLP, MLP-b does not interact with CFL2 as shown by blot overlay assays of MBP-MLP-a and MBP-MLP-b with GST-CFL2. (H–I) Competition

assays by blot overlay indicated that the presence of MLP-b does not affect the CFL2/MLP interaction.

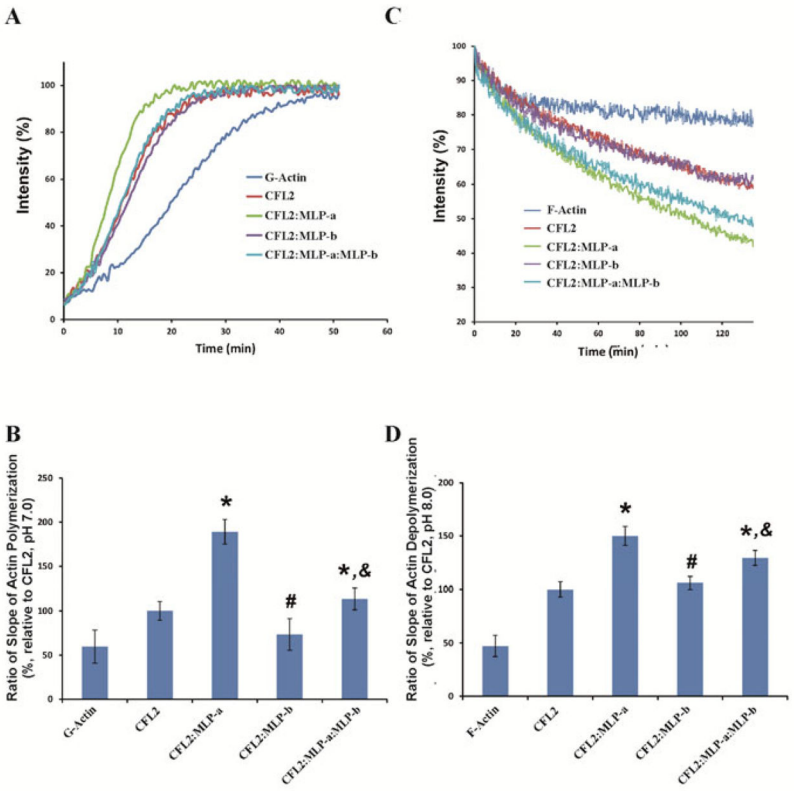

Fig. 7. MLP-b reduces the MLP enhancement of CFL2-mediated F-actin dynamics

(A) *In vitro* polymerization assays at pH 7.0 with suboptimal strength of actin polymerization buffer (0.25x) were performed in the presence of GST-CFL2, MBP-MLP-a and MBP-MLP-b. The molecular ratios CFL2:MLP-b and CFL2:MLP-a were 1:2, while the molecular ratio of CFL2:MLP-a:MLP-b was 1:2:1. MLP-a enhances the CFL2 F-actin severing activity, while MLP-b does not. (B) Calculation of the slope of G-actin polymerization of the different protein combinations. MLP-b diminishes the enhancing effect of MLP-a to CFL2 severing activity. (* CFL2:MLP-a vs CFL2, P=0.001, *t* test, two-tailed, n=3; # CFL2:MLP-b vs CFL2:MLP-a, P=0.001, *t* test, two-tailed, n=3; & CFL2:MLP-a:MLP-b vs CFL2:MLP-b, P=0.002, *t* test, two-tailed, n=3; # CFL2:MLP-a:MLP-b vs CFL2:MLP-a, P=0.03, *t* test, two-tailed, n=3) (C) *In vitro* depolymerization assays at pH 8.0 show how the presence of GST-CFL2, MBP-MLP-a and MBP-MLP-b affects F-actin over time. The molecular ratios CFL2:MLP-b and CFL2:MLP-a were 1:2, while the molecular ratio of CFL2:MLP-a:MLP-b was 1:2:1. MLP-b does not affect depolymerization of F-actin by CFL2 alone but in the presence of MLP-a. (D) Calculation of the slope of F-actin depolymerization of the different protein combinations. The slope of CFL2 and CFL2:MLP-b are comparative but the CFL2:MLP-a:MLP-b slope is approximately 20% lower than CFL2:MLP-a (* CFL2:MLP-a vs CFL2, P=0.001, *t* test, two-tailed, n=3; * CFL2:MLP-a:MLP-b vs CFL2, P=0.006, *t* test, two-tailed, n=3; # CFL2:MLP-b vs CFL2:MLP-a, P=0.002, *t* test, two-tailed, n=3; & CFL2:MLP-a:MLP-b vs CFL2:MLP-b, P=0.03, *t* test, two-tailed, n=3). Data are mean ± SEM.